ELSEVIER

Palaeogeography, Palaeoclimatology, Palaeoecology 133 (1997) 27–47

PALAEO

The Monte del Casino section (Northern Apennines, Italy): a potential Tortonian/Messinian boundary stratotype?

W. Krijgsman [a,*], F.J. Hilgen [b], A. Negri [c], J.R. Wijbrans [d], W.J. Zachariasse [b]

[a] *Paleomagnetic Laboratory, Fort Hoofddijk, Budapestlaan 17, NL-3584 CD Utrecht, The Netherlands*
[b] *Department of Geology, Institute of Earth Sciences, Budapestlaan 4, NL-3584 CD Utrecht, The Netherlands*
[c] *Department of Geology, University of Ancona, I-60128 Ancona, Italy*
[d] *Institute of Earth Sciences, VU Amsterdam, De Boelelaan 1085, NL-1007 MC Amsterdam, The Netherlands*

Received 1 April 1996; accepted 27 February 1997

Abstract

Results are presented from a high-resolution integrated stratigraphic study of the Monte del Casino section, which is considered as a candidate boundary stratotype section for the Tortonian/Messinian (T/M) boundary. The section yields a good to excellent cyclostratigraphy, tephrastratigraphy and planktonic foraminiferal and nannofossil biostratigraphy. It can be correlated in detail to other Mediterranean sections using cyclostratigraphic patterns in combination with the planktonic foraminiferal biostratigraphy. These correlations indicate that the succession of the Monte del Casino composite section is continuous in the T/M boundary interval and that all sedimentary cycles, volcanic ash layers and bio-events can be accurately dated by tuning the sedimentary cycles to astronomical target curves.

The quality of the paleomagnetic signal varies considerably throughout the section. A reliable magnetostratigraphy cannot be established for the T/M boundary interval because of a secondary magnetisation carried by iron sulphides. Cyclostratigraphic correlations indicate that discrepancies exist between the position of the reversals recorded here and those found in earlier magnetostratigraphic studies. Comparison of $^{40}Ar/^{39}Ar$ ages of ash layers with their astronomical ages, show that biotite ages give a good approximation of the age of the section, but are not suitable for high-resolution chronology. Despite these short-comings the Monte del Casino section remains a candidate to define the T/M boundary, but its qualities should be critically weighted against those of other sections. © 1997 Elsevier Science B.V.

Keywords: $^{40}Ar/^{39}Ar$ dating; astronomical dating; calcareous plankton biostratigraphy; Northern Apennines; paleomagnetism; Tortonian/Messinian boundary

1. Introduction

The Tortonian/Messinian (T/M) boundary is at present defined at the first occurrence level of *Globorotalia conomiozea* in the Falconara section on Sicily (Colalongo et al., 1979). Subsequent studies revealed however that this section is unsuitable to define this boundary according to criteria formulated by the International Commission on Stratigraphy (Cowie et al., 1986): the section is completely remagnetised (Langereis and Dekkers, 1992) and seriously deformed tectonically in the

* Corresponding author.

PII S0031-0182(97)00039-4

critical interval (field observations and unpublished data). Better sections for defining the T/M boundary stratotype are to be found on Crete and Gavdos, in Morocco and in northern Italy.

The Potamida and Faneromeni sections on Crete and the Metochia section on Gavdos have yielded a good to excellent magnetostratigraphy, planktonic foraminiferal biostratigraphy and cyclostratigraphy (Langereis et al., 1984; Krijgsman et al., 1994, 1995). The polarity sequence only recently allowed a straightforward and unambiguous calibration to the Geomagnetic Polarity Time Scale (GPTS) of Cande and Kent (1992, 1995). All sections are correlated in detail using sedimentary cycle patterns in combination with the magnetostratigraphy and a high-resolution planktonic foraminiferal biostratigraphy (Krijgsman et al., 1995). Calibration of the cycle patterns to astronomical target curves resulted, among others, in an age of 7.24 Ma for the T/M boundary (Hilgen et al., 1995).

The Oued Akrech section in Morocco (Benson et al., 1991; Benson et al., 1995) has the advantage that it is located at the Atlantic side of the Riffean corridor, thus facilitating correlations to the open ocean. The section has provided a good paleomagnetic signal and shows a distinct cyclic bedding (Benson et al., 1995; own field observations). It therefore has the potential to be correlated to the astronomical solutions (see also Benson et al., 1995).

Vai et al. (1993) proposed the Monte del Casino section in northern Italy as a potential alternative type section, even though this section is tectonically deformed and a reliable magnetostratigraphy is lacking (Negri and Vigliotti, 1997). A clear advantage of this section is the large number of biotite-rich ash layers. Radiometric dating of these ash layers resulted in an age of 7.07 ± 0.05 Ma for the T/M boundary (Vai and Laurenzi, 1994). There are, however, problems in correlating the sedimentary cycles from Monte del Casino I to Monte del Casino II, and to the Monte Tondo section located 8 km to the SE (Vai et al., 1993). This unsuitability of the sedimentary cycle patterns for high-resolution time-stratigraphic correlations is in contrast to results of integrated stratigraphic studies of coeval marine sections on Crete and Sicily (Krijgsman et al., 1994, 1995). Therefore, we decided to study the Monte del Casino section in detail. The aim of this study is two-fold: firstly, to test the cyclostratigraphic, biostratigraphic and magnetostratigraphic potential of this section, and secondly, to compare the radiometric ($^{40}Ar/^{39}Ar$) ages of the volcanic ash layers with astronomically derived ages for the same events. We determined $^{40}Ar/^{39}Ar$ ages of several ash layers ourselves in addition to the ages made already available by Laurenzi et al. (1997). Finally, all results will be used to evaluate critically the Monte del Casino section as a potential T/M boundary stratotype.

2. Sections

The Monte del Casino and Monte Tondo sections are situated 8 km apart, in the foothills of the Northern Apennines (Fig. 1). Both sections consist of open marine grey to blue coloured marly clays with numerous intercalations of biotite-rich ash layers and brown to black coloured, organic-rich, laminated sediments termed sapropels (Calieri, 1992; Vai et al., 1993). The clays are of late Tortonian–early Messinian age, overlie turbidites of the Formazione Marnoso-Arenacea and are

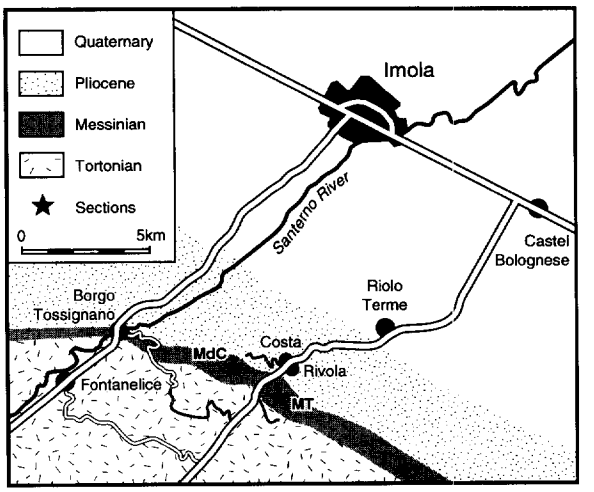

Fig. 1. Location map of the Monte del Casino (*MdC*) and Monte Tondo (*MT*) sections in the Vena del Gesso basin of the Northern Apennines (Italy).

overlain by Messinian limestones of the Calcare di Base and gypsum of the Lower Evaporites.

In the present study, we focus on the stratigraphic interval which straddles the T/M boundary (Fig. 2). We studied essentially the same interval as Vai et al. (1993) but did not include the deformed top part of the section. The section can be extended downward to reach the turbidites. This extension contains an additional 14 sapropels, but is not included in the present study. For this reason, the first sapropel in the lithological log is numbered C15.

Discrete low-angle shearplanes between C15 and ash 104a seriously disturb the stratigraphic continuity. The deformation was almost completely avoided in our composite section (see Fig. 3). The middle part of the section, including the T/M boundary interval, is relatively undisturbed. Deformation — in the form of bedding parallel shearplanes — becomes again more intense towards the top of the section (from C40 onwards). In comparison with Monte del Casino, the Monte Tondo section is tectonically more strongly deformed. Like at Monte del Casino, deformation is related to NE-ward directed thrusting in combination with the presence of competent stratigraphic units higher in the succession (i.e. the gypsum evaporites).

3. Cyclostratigraphy and tephrastratigraphy

The succession shows a distinct cyclic bedding. Sedimentary cycles typically consist of a grey to blue coloured homogeneous marly clay (lithofacies A1 of Vai et al., 1993) and a brown to black coloured, laminated layer which is enriched in organic matter and termed sapropel (E1). A distinct grey non-laminated layer is found on top of most sapropels (E2). Sapropels are not found throughout the section, but occur in distinct intervals. Three lower sapropels (C15–C17) are

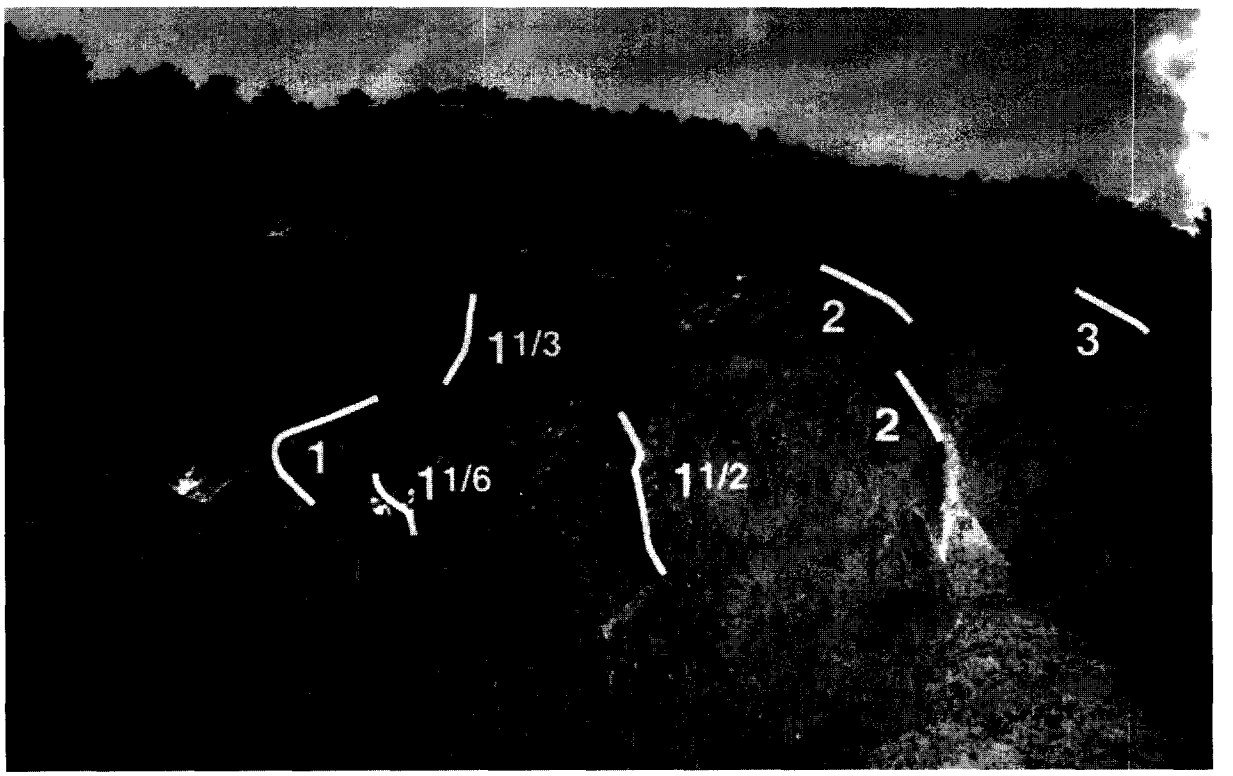

Fig. 2. Photograph of the Monte del Casino section showing sampling trajectories of subsections (see also Fig. 3).


hom. clay
ash layer
dark clay
sapropel
Casino 1
Casino 1⅓
Casino 1⅙
Casino 1½
Casino 2
Casino 2
Casino 3
M.Tondo
gci
gn
gs
gc
am
cp
m4
m5
f
2.0
1.0
0m.
1.0
0.5
0m.

followed by a thick homogeneous interval. This homogeneous interval is in turn succeeded by a regular and cyclic alternation of sapropels and clays which continues to the top of the section. In this upper part, some characteristic cycle patterns can be distinguished in addition to the basic cyclic repetition. Cycles with distinct sapropels (C18, C20 and C22) alternate with cycles in which sapropels are weakly developed (C21) or even absent (C19). Sapropels are further absent in cycles C26, C33 and C34. The homogeneous bed of cycle C29 is anomalously thick. The homogeneous bed of C41 is very prominent and distinctly white coloured.

Our cyclostratigraphic log deviates in detail considerably from the logs presented by Vai et al. (1993). Vai et al. (1993) did not succeed to correlate their Monte del Casino I and II sections cyclostratigraphically, despite the fact that these sections are located only 50 m apart. This is not unexpected since our field observations revealed serious deformation in parts of both their trajectories. However, deformation was almost completely avoided in our composite section, which therefore represents an obvious improvement.

The Monte del Casino section contains 19 biotite-rich layers which appear as mm- to 1-cm-thick partings (Fig. 3). In addition to abundant biotite flakes, these layers contain labradoritic plagioclase and quartz (Vai et al., 1993; Laurenzi et al., 1997). Disperse biotite flakes are found in a 4–6-cm-thick sedimentary interval straddling the ash layers. Biotite crystals are well-preserved with an idiomorphic hexagonal outline, suggesting a volcanic origin as fallout deposits (Vai et al., 1993). The numbering of the ash layers is after Laurenzi et al. (1997); newly found layers are given the extension a,b, etc.

4. Biostratigraphy

4.1. Planktonic foraminifera

Planktonic foraminiferal biostratigraphy of the Monte del Casino composite section is based on the semi-quantitative distribution of 5 taxa plus the coiling ratio of non-keeled globorotaliids in 130 samples (Fig. 4). Additional samples were qualitatively analysed from overlapping parts of the Monte del Casino (sub)sections and from Monte Tondo to check cyclostratigraphic and tephrastratigraphic correlations (Fig. 3).

Keeled globorotaliids provide the most useful biostratigraphic events (Fig. 4). A short but prominent influx of the left-coiled *Globorotalia menardii 4* occurs around sapropel C16. Keeled globorotaliids then become absent again up to the first occurrence (FO) level of the right-coiled *Globorotalia menardii 5* directly below ash 104b. The interval in which *G. menardii 5* is the dominant keeled globorotaliid is punctuated by a very short but distinct influx of *G. menardii 4* slightly above ash 105. At ash layer 106, *G. menardii 5* is definitively replaced by left-coiled assemblages of keeled globorotaliids characterised by a reniform chamber outline in spiral view. These assemblages are termed the *Globorotalia conomiozea* group by Zachariasse (1979) and the *Globorotalia miotumida* group by Sierro (1985) and Sierro et al. (1993). Although the earliest representatives of the *G. conomiozea* group usually show flat tests typical of *G. miotumida*, the first sample directly above 106 already contains an assemblage that is dominated by conical forms usually labelled as *G. conomiozea*, *G. conoidea*, *G. saphoa* or *G. mediterranea*. The next sample dominated by these conical

Fig. 3. Monte del Casino subsections are found in the different gullies of the bad-land exposure. Casino 1 is located directly SE of Monte del Casino I of Vai et al. (1993) whereas Casino 2 corresponds to (part of) Monte del Casino II of Vai et al. (1993). Where possible lateral tracing of marker-beds was used to physically correlate subsections. The correlation between the subsections of Monte del Casino $1\frac{1}{3}$ and 2 is based on the sedimentary cycle pattern in combination with the position of ashes 107 and 108; between Casino 1 and $1\frac{1}{6}$ on sedimentary cycle patterns and the relative position of ashes 103, 104a, 104b and 105; between Casino 1 and $1\frac{1}{3}$ (ash 107); Casino $1\frac{1}{2}$ and $1\frac{1}{6}$ (ash 104b), Casino $1\frac{1}{2}$ and 2 (ashes 102 and 103; sapropels C15 and C16) and Casino 2 and 3 (ash 103). These correlations are indicated by *solid lines* connecting the different subsections. The position of samples and bio-events have been indicated: m4 = *G. menardii 4*; m5 = *G. menardii 5*; gc = *G. conomiozea*; gci = influxes of *G. conomiozea* s.s.; gs = *G. scitula* group; gn = *G. nicolae*; cp = *C. parvulus*; and am = *Amaurolithus* spp. Numbering of ash layers is after Laurenzi et al. (1997); newly found ash layers have been given an extension a, b, etc. The Monte del Casino composite section is indicated by the samples connected by the *thick line*. Sapropels and grey beds have been numbered — from 15 to 41 — in stratigraphical order.

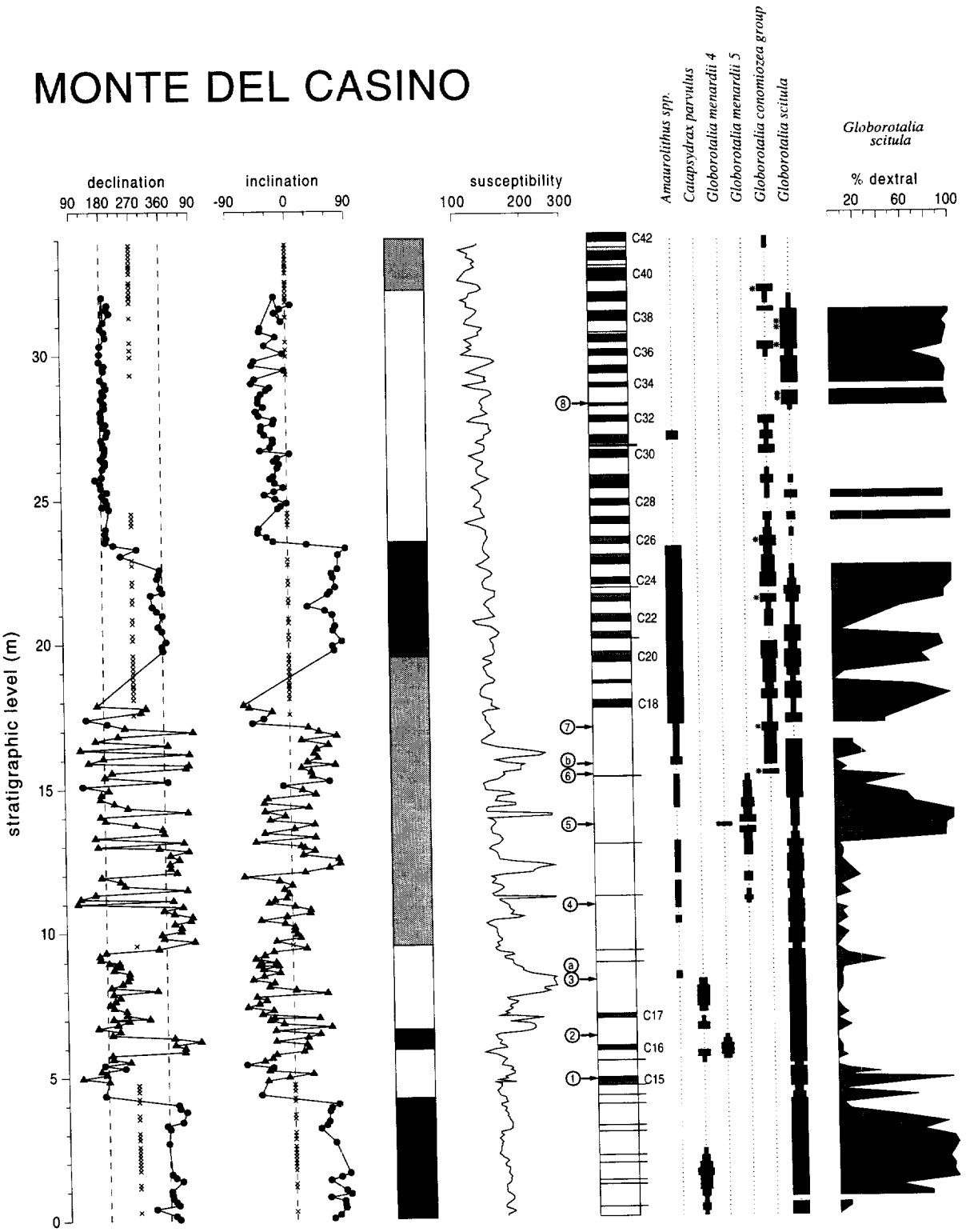
MONTE DEL CASINO
declination
90 180 270 360 90
inclination
-90 0 90
susceptibility
100 200 300
Amaurolithus spp.
Catapsydrax parvulus
Globorotalia menardii 4
Globorotalia menardii 5
Globorotalia conomiozea group
Globorotalia scitula
Globorotalia scitula
% dextral
20 60 100
stratigraphic level (m)
0
5
10
15
20
25
30
C42
C40
C38
C36
C34
C32
C30
C28
C26
C24
C22
C20
C18
C17
C16
C15
8
7
b
6
5
4
a
3
2
1

forms is found higher up in the succession, below sapropel C18. A last major influx of the *G. conomiozea* group is found in cycle 39 (Fig. 4).

Coiling changes of the unkeeled globorotaliids, collectively labelled the *G. scitula* group, provide some additional bio-events. A persistent change in coiling direction — from dextral (via mixed dextral/sinistral) to sinistral — coincides with sapropel C15. Dominantly left-coiling assemblages are found to a level approximately 1 m above ash 105 (Fig. 4). This level corresponds to the middle part of the range of *G. menardii 5*. The coiling direction then switches back to an alternating mode. Dominantly right-coiling representatives of the *G. scitula* group are intermittently found in low numbers from sapropel C23 upwards but become abundant again from the grey bed of cycle 33 to sapropel C38. Bottom and top of this interval correspond with the FO and LO (last occurrence) of *G. nicolae*, respectively, a dextrally-coiled and biconvex form with inflated chambers of the *G. scitula* group. The FO of *G. nicolae* thus follows a relatively long interval in which unkeeled globorotaliids are rare or absent (Fig. 4).

Another useful bioevent is the LO of *Catapsydrax parvulus*. This event is found above sapropel C17. Neogloboquadrinids show dominant left coiling throughout the section. A change in coiling direction (i.e. from sinistral to dextral) has been reported by Vai et al. (1993) from a level well above the top of our section.

4.2. Calcareous nannofossils

Preparation of the calcareous nannofossil samples followed standard techniques: no centrifugation was done to retain the original composition in the assemblage and a smear slide was mounted with Norland optical adhesive. Analyses were done according to the semi-quantitative methodology of Rio et al. (1990), to define the FO of the *Amaurolithus* group. Nannofossil counts are based on surveying a standard number of fields (1000) using a light microscope with 1250× magnification. All samples show an abundant and moderately to well-preserved nannoflora. In general, the best preserved nannoflora occur in sapropel layers together with abundant pyrite. The assemblage mainly consists of *Reticulofenestra* spp. with many levels showing abundant "small" (less than 3 μm) *Reticulofenestra* spp., *R. pseudoumbilicus*, *Coccolithus pelagicus*, (specimens of 7–10 μm), *Sphenolithus moriformis* and *S. abies*. Further, *Syracosphaera pulchra*, *Syracosphaera* spp., *Triquetrorhabdulus rugosus*, *Rhabdosphaera* spp. and *Scyphosphaera* spp. are commonly recorded. *Reticulofenestra rotaria* is rare in the higher part of the section.

The genus *Discoaster* is generally abundant, but preservation varies from very poor to good; again, the best preserved specimens occur in sapropel layers. Most of the specimens belong to *D. variabilis* and *D. pentaradiatus*. *Discoaster brouweri* and *D. intercalaris* are commonly recorded, while *D. challengeri* and *D. icarus* are rare. In the lower part of the section few specimens of *D. loeblichii* have been observed. Furthermore, *D. tamalis* and *D. asymmetricus* are observed. Both species are usually found in the early Pliocene (the FO of *D. asymmetricus* marks the base of the NN 14 zone

Fig. 4. Polarity zones, susceptibility, lithology, cycle numbers and ranges of planktonic foraminifera of the Monte del Casino section. In the polarity column *black* and *white* denote normal and reversed polarity interval, respectively, and *shaded interval* denotes zone of undefined (only secondary components) polarity. *Solid dots* represent directions from demagnetisation diagrams showing a gradual decrease of the magnetisation up to temperatures of 420°C carried by magnetite, and *triangles* from diagrams showing a rapid decrease between 300° and 360°C carried by iron sulphide directions (see text). *Crosses* denote samples for which directions could not be ascertained because of extremely low intensities. Lithology column shows cyclic alternations of homogeneous marls/marly clays (*white*) and sapropels (*black*); *shaded interval* represents grey layers. Biostratigraphic data of planktonic foraminiferal marker species are based on surveying a standard number of fields (27 out of 45) on a rectangular picking tray and semi-quantitatively presented in terms of absence: trace (<3 specimens per 9 fields of picking tray), rare (3–10), common (10–30) and frequent (>30) indicated by increasing bar thickness. Calcareous plankton events indicated are: (1) dextral to sinistral coiling change of *G. scitula* group, (2) Last Common Occurrence of *G. menardii 4*, (3) Last Occurrence of *C. parvulus*, (4) First Occurrence of *G. menardii 5*, (5) *G. menardii 4* influx and Last Occurrence, (6) First Regular Occurrence (FRO) of the *G. conomiozea* gr., (7) influx of conical *G. conomiozea*, (8) First Occurrence of *G. nicolae*, (a) First Occurrence of *Amaurolithus* spp. and (b) First Common Occurrence of *Amaurolithus* spp. *Arrows* indicate positions of bioevents.

of Martini (1971), and the FO of *D. tamalis* is recorded by Perch Nielsen (1985) in the NN 15 zone) but have also been reported from the Late Miocene (e.g., Bukry, 1973).

The genus *Helicosphaera* is well presented by *H. carteri* and *H. intermedia*. *H. orientalis*, *H. stalis* and *H. walbersdorfensis* (the "small" Helicosphaera group according to Negri and Vigliotti, 1997) are almost continuously recorded in the lower part of the section, but become more scattered towards the top.

The occurrence of the genus *Amaurolithus* is rare and discontinuous, especially in the early part of its range. The FO of *Amaurolithus* spp. is recorded between 8.13 and 8.37 m, i.e. well below ash 104 (Fig. 4). Rare *A. primus* and *A. amplificus* are recorded discontinuously in the interval between 8.37 and 15.56 m. Between 15.81 and 23.07 m, *Amaurolithus* spp. is more abundant and continuous, and consists mainly of *A. delicatus*. Representatives of this group become scattered again from 24.55 m to nearly absent toward the top of the section. This pattern has also been recorded in the Monte Tondo section (Negri and Vigliotti, 1997) and probably allows to discriminate two events in the *Amaurolithus* group: (a) the FO and (b) an interval in which this Amaurolithus is particularly frequent, probably caused by favourable environmental conditions in the basin (Fig. 4).

5. Magnetostratigraphy

5.1. Methods

To establish the magnetostratigraphy for the Monte del Casino section, 269 levels were sampled and at least one specimen per sampling level was thermally demagnetised. Thermal demagnetisation was applied with small temperature increments of 20–30°C up to a maximum temperature of 420°C, in a magnetically shielded, laboratory-built, furnace. The natural remanent magnetisation (NRM) was measured on a 2G Enterprises DC SQUID cryogenic magnetometer. Furthermore, several rock magnetic experiments were performed to identify the carriers of the magnetisation. The initial susceptibility and the anisotropy were measured on a Kappabridge KLY-2. An isothermal remanent magnetisation (IRM) was acquired on a PM4 pulse magnetiser up to a maximum field of 2000 mT. The IRM was subsequently thermally demagnetised, and after each temperature step the bulk susceptibility was measured. Finally, thermomagnetic runs were recorded with a modified horizontal translation Curie balance making use of a cycling field (Mullender et al., 1993).

5.2. Thermal demagnetisation

Throughout the whole section, thermal demagnetisation diagrams are of mixed quality. Fortunately, the relatively large dip (40°) of the section was useful to distinguish between primary and secondary components.

The lowermost part of the section (0–4 m) predominantly shows normal polarities after bedding plane correction (Figs. 4 and 5A). NRM-intensities generally range from 0.1 to 1 mA/m. The remanence is usually gradually removed at temperatures below 400°C. Further demagnetisation at higher temperatures results in a mainly randomly directed viscous component. Several samples in this interval have very low NRM intensities (<0.05 mA/m) and their directions and polarities could not be determined (Figs. 4 and 5B).

The following interval (4–9.5 m) mainly shows reversed polarities, except for several samples between 6 and 7 m (Figs. 4 and 5C, D). Demagnetisation diagrams show that a normal polarity component is removed at temperatures below 240°C and a reversed component between 240° and 360°C. The low-temperature component has a present-day field direction before bedding plane correction and can thus be regarded as a secondary overprint, probably caused by subrecent weathering. In some cases this overprint is even absent, indicating that we sampled in fresh (unaltered) sediments (Fig. 5E). Thermal demagnetisation between 100° and 300°C only removes a small part of the NRM. At temperatures between 300° and 360°C, a large decrease in the remanence is observed. This indicates the presence of a magnetic carrier with a Curie point slightly above 300°C, probably an iron sulphide like greigite or pyrrho-

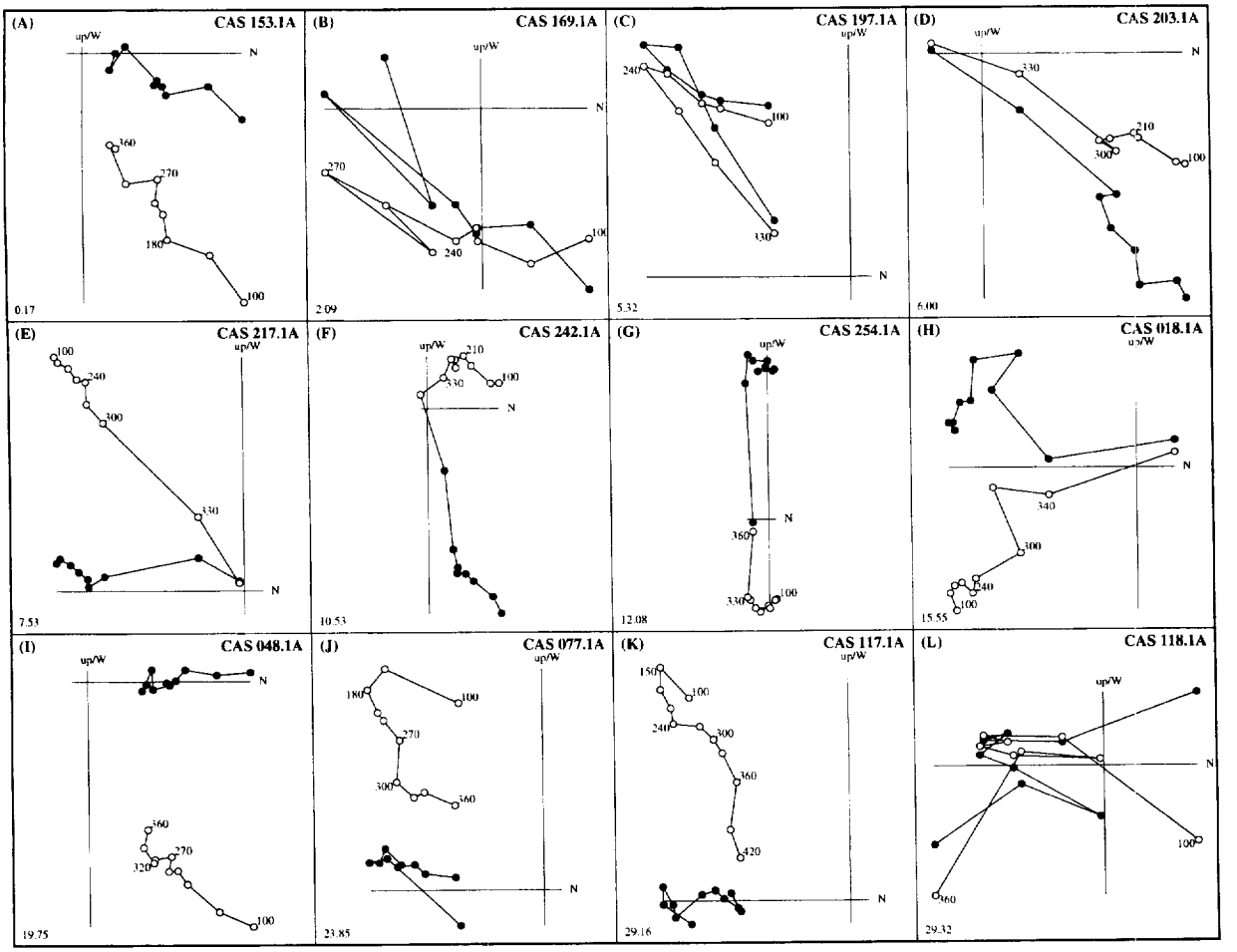

Fig. 5. Thermal demagnetisation diagrams for samples of the Monte del Casino section. *Closed* ad *open symbols* represent the projection of the vector end-points on the horizontal and vertical plane, respectively; values represent temperatures in °C; stratigraphic levels are in lower left-hand corner.

tite. Demagnetisation at temperatures higher than 360°C, mainly shows viscous components.

The middle part of the section (9.5–19.5 m) shows the same type of demagnetisation behaviour, but NRM intensities are much higher (1–10 mA/m) and most directions are neither normal nor reversed (Figs. 4 and 5F–H). The latter indicates a secondary (diagenetic) origin of the magnetisation in this part of the section.

In the upper (cyclic) part of the section (19.5–32 m), NRM intensities range from 0.05 to 1 mA/m. Demagnetisation diagrams are mostly of good quality, especially in the homogeneous intervals (Figs. 4 and 5I–K). Generally, a secondary present-day field component is removed below 180°C. Demagnetisation at higher temperatures reveals a gradual removal of the magnetisation up to temperatures of 420°C. This indicates that the contribution of magnetic iron sulphides is negligible in this part of the section. Remarkably, in some cases, the diagrams give a much better defined reversed component without bedding plane correction. In several of the sapropelic beds and in the uppermost part of the section (32–34 m),

the NRM is very low. Reliable directions could not be ascertained from these samples and demagnetisation diagrams only show scatter (Fig. 5L).

5.3. Rock magnetic results

The IRM acquisition curves indicate the presence of two different components (Fig. 6A). A general steep rise between 0 and 100 mT and saturation at 200 mT indicates the presence of a low-coercivity mineral like magnetite or maghemite. These curves are characteristic for samples of the upper and lowermost part of the section. Samples from the middle part show a less prominent rise at the lowest fields (0–50 mT) and saturation at approximately 500 mT, suggesting the presence of iron sulphides.

In a few samples, three orthogonal IRM compo-

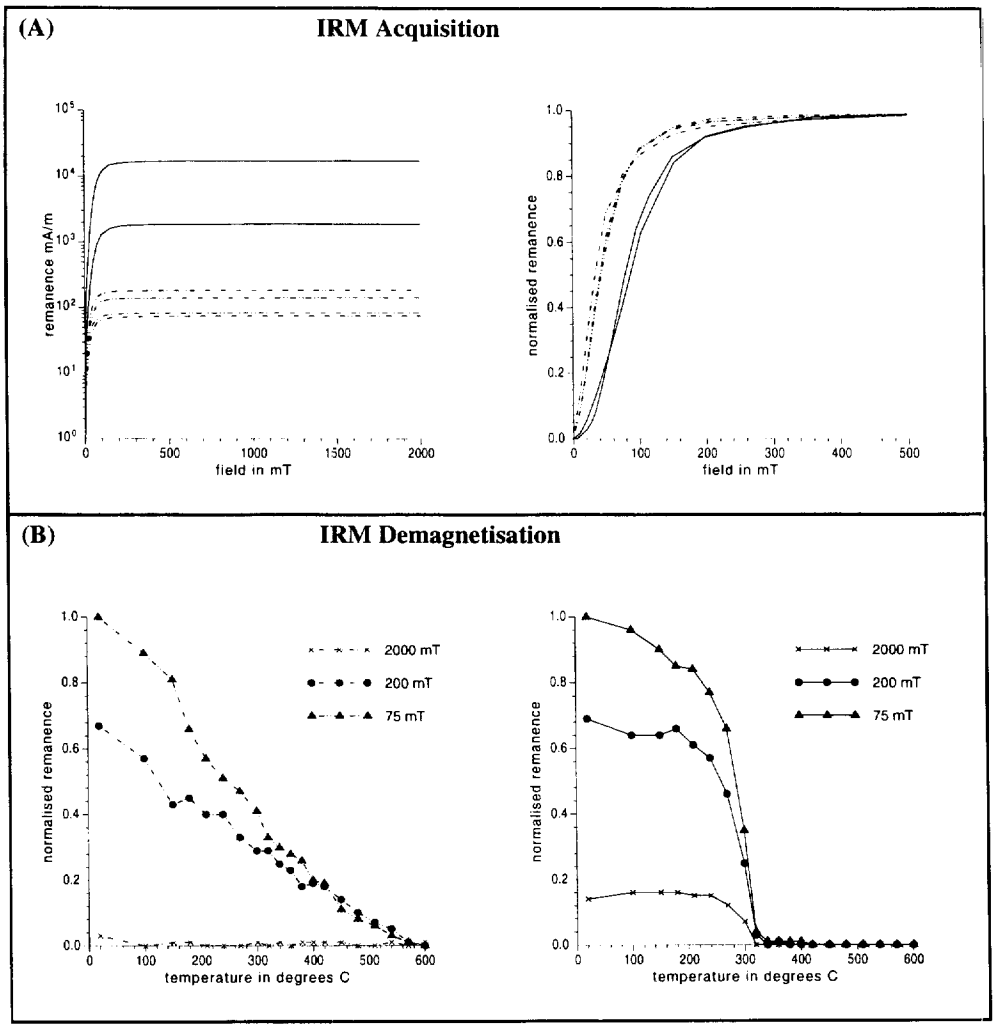

Fig. 6. A. Examples of IRM acquisition of samples of the Monte del Casino section. The initial steep rise points to magnetite, the gradual increase at lowest fields suggests the presence of iron sulphides like pyrrhotite or greighite.

B. Stepwise thermal demagnetisation of the normalised three-axial IRM also shows the presence of both iron sulphides and magnetite.

In both (A) and (B), *dotted lines* represent magnetite dominated samples, *solid lines* iron sulphide dominated samples.

nents were induced according to the method of Lowrie (1990) (Fig. 6B). The demagnetisation of this composite IRM confirms the presence of two magnetic components. The low-coercivity dominated samples show an unblocking temperature of 580°C, which is characteristic for magnetite (Fig. 6B). The higher-coercivity dominated samples show a strong decrease at temperatures between 240° and 320°C, which is indicative for iron sulphides which have Curie temperatures of 320–325°C for pyrrhotite (Dekkers, 1989) and 333°C for greigite (Spender et al., 1972; see also Roberts, 1995).

During thermal demagnetisation of the IRM we also measured the bulk susceptibility after each temperature increment (Fig. 7A). No significant changes in the susceptibility are observed below 380°C. Heating to higher temperatures results in a large increase of susceptibility which continues up to temperatures of 450°C. This behaviour was observed earlier in sediments from suboxic to anoxic environments and is likely the result of oxidation of pyrite (Van Velzen, 1993). The subsequent decrease in susceptibility between 450° and 600°C can be ascribed to oxidation of magnetite to hematite. The thermomagnetic runs partly confirm these observations, but show an increase in magnetisation at temperatures of 420°C, thus slightly higher than in the susceptibility records (Fig. 7B). The 350°C run shows a (weakly developed) Curie point at approximately 320°C, suggesting that the iron sulphide is pyrrhotite, because greigite would begin to break down above 282°C (Skinner et al., 1964; Roberts, 1995) and has, in addition, a slightly higher Curie temperature of 333°C (Spender et al., 1972).

5.4. Susceptibility and anisotropy

The initial susceptibility (χ_{in}) of the sediment is strongly dependent on the concentration of paramagnetic clay minerals. The results from the Monte del Casino section show that a clear relation with the cyclicity exists in the upper part of the section (Fig. 4). The lowest values of χ_{in} are dominantly observed at the bottom of the sapropels, the highest values at the bottom of the homogeneous marls; at the top of the grey intervals.

The anisotropy of the magnetic susceptibility (AMS) can be used to provide information on the tectonic deformation of the sediment (Kissel et al., 1986; Scheepers, 1994). There is often a clear relation between the AMS and the regional stress field in the area; a magnetic lineation may develop perpendicular to the regional stress field. The anisotropy at Monte del Casino (determined for 30% of the samples) is generally 1–2%. After bedding plane correction, the minimum axes are

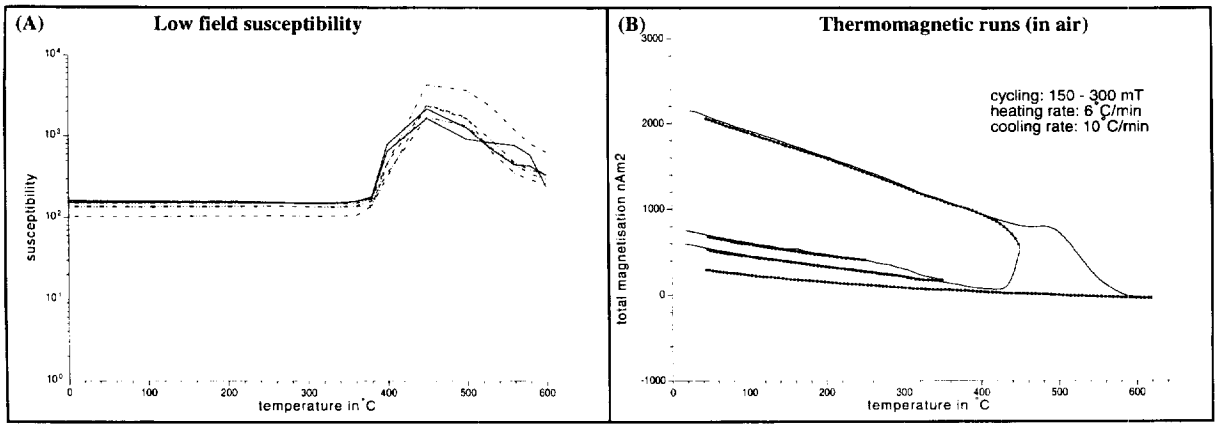

Fig. 7. A. Low-field susceptibility during thermal demagnetisation; the increase in susceptibility between 400° and 500°C is probably related to the oxidation of pyrite to magnetite.

B. Example of a thermomagnetic run in air showing a faint Curie point at a temperature of 320°C, suggesting the presence of pyrrhotite.

all vertical, the intermediate and maximum axes are randomly oriented in the horizontal plane (Fig. 8). Furthermore, it shows that the fabric causing the anisotropy is entirely foliated (oblate). Some degree of lineation is observed in the tectonically disturbed interval between sapropels C15 and C17. The tectonic deformation at Monte del Casino obviously had no major influence on the magnetic fabric. The strong oblateness of the fabric, and the absence of lineation, indicates that deposition had taken place on a horizontal plane in a very quiet sedimentation environment.

6. Ar/Ar dating

6.1. Methods

Argon geochronology was carried out using laser fusion and incremental heating techniques. A detailed description of techniques was published earlier (Wijbrans et al., 1995); here we describe the sample preparation and experimental conditions pertinent to this study. The ash layers contain well-preserved euhedral biotite crystals and a slightly milky feldspar fraction. From the biotites, we separated the largest crystal fraction (250–500 μm). In cases where the yield in this size fraction was insufficient, a smaller crystal fraction (125–250 μm) was added. The feldspar fraction was prepared using standard heavy-liquid and magnet separating techniques. For the Monte del Casino ashes, the feldspar fractions consisted mainly of plagioclase. For both the plagioclase and the biotite, approximately 20-mg aliquots were packaged in Al foil, and loaded in a 5-mm-ID quartz tube with the flux monitors (USGS standard 85G003 TCR sanidine, K/Ar age 27.92 Ma) packaged in Cu foil. Individual packages were approximately 1 mm thick, and standards were loaded between each set of 5 unknowns. Irradiation with fast neutrons was carried out in the CLICIT facility in the Oregon State University TRIGA reactor (Dodd and Anderson, 1994).

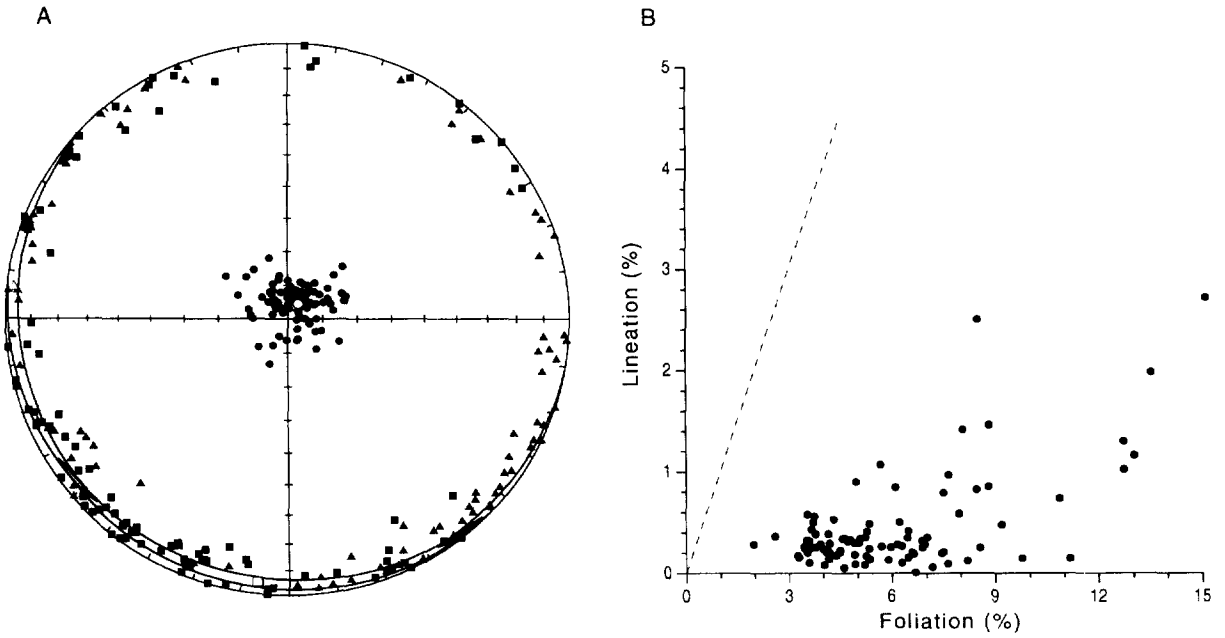

Fig. 8. Anisotropy of the initial susceptibility.

A. Principal axis of the anisotropy; *dots* denote minimum axis, *triangles* maximum axis and *squares* intermediate axis. *Open symbols* denote the mean direction of the principal axes.

B. Flinn diagram showing lineation versus foliation. The magnetic fabric is oblate which indicates that deposition has taken place on a horizontal plane in a quiet sedimentary environment without any currents.

After irradiation, the samples were loaded in a Cu tray (60 mm diameter) with 2-mm-diameter holes for each individual experiment. For both the standards and the unknowns, we applied a single fusion technique where for each sample 5 replicates (>1.0 mg each) were analysed. The biotites and plagioclase samples were preheated to approximately 500°C in order to remove some of the atmospheric argon that interferes with accurate analysis of the radiogenic argon component in young samples. In addition, biotites MCA-1 and MCA-2a were analysed using an incremental heating technique, using a defocussed laser beam and stepping up of the power of the laser beam for each subsequent degassing step until fusion of the biotite sample occurred.

The argon gas was measured isotopically using a double focussing noble gas mass spectrometer (MAP215-50) in static mode. Beam intensities were measured on a secondary electron multiplier detector (gain 60,000) and switchable preamplifier resistor settings (109, 108 and 107Ω) by peak jumping at half mass intervals down from mass 40 to 35.5. System blanks were measured at least between every set of 5 unknowns. In general, the blank correction was the average of the blanks run before and after the unknown. System blanks in a laser fusion system tend to be predictable and usually show a slight increase during the day. For the main isotopes ^{40}Ar and ^{39}Ar, sample to blank ratios were always less than 100. The blanks for this project were typically in the range *m/e*:40 $(6.0–2.0)\times10^{-16}$ mol, *m/e*:39 $(3.0–1.5)\times10^{-17}$ mol, *m/e*:38 $(2.0–1.0)\times10^{-17}$ mol, *m/e*:37 $(2.5–2.0)\times10^{-16}$ mol, *m/e*:36 $(4.0–3.0)\times10^{-17}$ mol. System mass discrimination was measured by letting clean air argon (approximately 5.0×10^{-14} mol ^{40}Ar) into the mass spectrometer from a 10-l reservoir using a 1-ml gas pipette.

For the age spectra, the plateaus meet commonly used criteria (Fleck et al., 1977). The plateau ages are calculated as the weighted mean of the individual steps using the inverse of the variance of the $^{40}Ar/^{39}Ar$ ratio as the weighting factor. The uncertainties are quoted at the 1σ level.

6.2. Results

The results of argon dating are summarised in Table 1, the age spectra for MCA-1 and -2a are given in Fig. 9. Apparently, weighted mean ages of single fusion datings do not match the stratigraphic order, while in addition discrepancies exist between biotite and plagioclase ages for the same

Table 1
Argon ages of ash layers

Sample	Mineral	$^{40}Ar/^{39}Ar$	Isochron	*n*	MSWD
MCA-9	biotite	7.30±0.05	7.27±0.06	3	1.64
	plagioclase	7.89±0.07	8.17±0.08	4	1.70
MCA-3	biotite	7.70±0.03	7.27±0.08	5	20.9
	plagioclase	7.48±0.05	7.41±0.04	4	2.79
MCA-2a	biotite	7.49±0.01	7.51±0.03	5	1.28
	B-plateau	7.56±0.07	7.51±0.02	9	0.07
	plagioclase	9.55±0.07	7.17±0.09	4	23.3
MCA-1	biotite	7.53±0.01	7.30±0.10	4	1.06
	B-plateau	7.48±0.02	7.58±0.05	13	0.02
	plagioclase	8.34±0.12	7.46±0.18	3	3.12
MCA-0	biotite	7.47±0.02	7.32±0.15	4	2.07

The age monitor used for these experiments was the USGS standard 85G003 TCR sanidine, with an age of 27.92 Ma. *n* represents the number of points used in regression; MSWD the quality of fit.

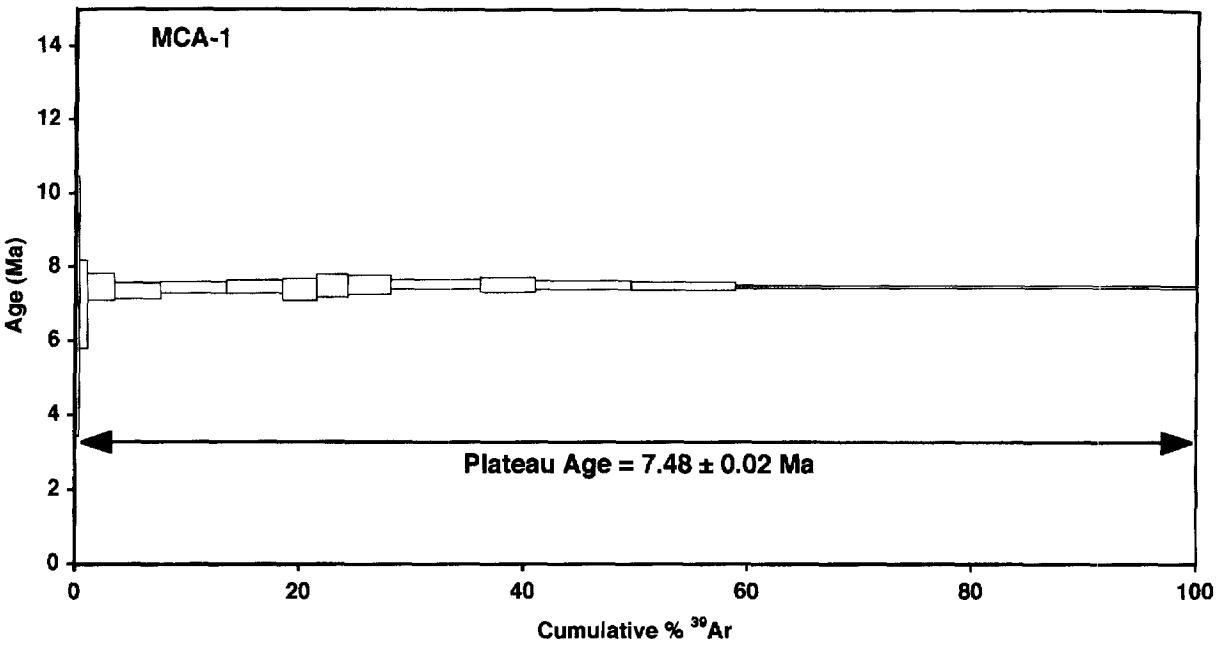

(a)

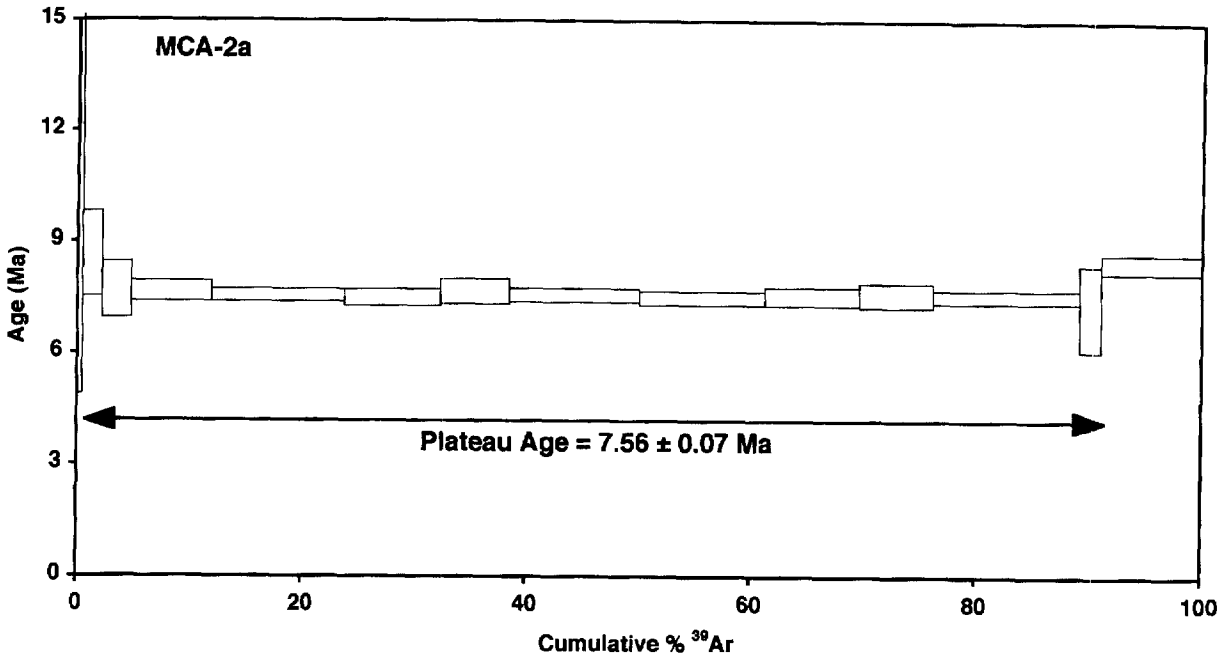

(b)

Fig. 9. $^{40}Ar/^{39}Ar$ age spectra for biotite samples of ash layers 102 (MCA-1) and 103 (MCA-2a). The age monitor used for these experiments was the USGS standard 85G003 TCR sanidine, with an age of 27.92 Ma. For the age spectra, the plateaus meet commonly used criteria (Fleck et al., 1977). The plateau ages are calculated as the weighted mean of the individual steps using the inverse of the variance of the $^{40}Ar/^{39}Ar$ ratio as the weighting factor. The uncertainties are quoted at the 1σ level.

level. Biotite ages are all in the same range, whereas in some cases plagioclase ages are considerably older. These plagioclase ages appear to be affected by varying amounts of excess argon.

It is commonly assumed that before eruption silicic magmas contain fluids that include some argon, but in many cases most of this fluid is liberated during extrusion, effectively resetting the argon geochronometer. Our data show that degassing of the plagioclase during eruption of the magma was not complete. As plagioclase contains less K than biotite, the effect of incorporation of excess argon in plagioclase is more dramatic, but we must assume that the biotite ages are affected to some degree as well.

In argon geochronology there are two techniques that may help to assess the effects of excess argon in the system. When the isotopic data are regressed in an isotope correlation diagram, no assumptions are made concerning the isotopic composition of the non-radiogenic component on the argon gas. It can be seen (Table 1), that for the plagioclase samples the regression ages are mostly younger than the mean age of the single fusion experiments, confirming the presence of excess argon. The relatively large uncertainty of the regression ages prevents us from using these age for high-resolution chronology. The biotite regression ages also tend to be slightly younger than the mean of the single fusion ages, which is consistent with the presence of some excess argon in the biotites, although the effect is so small that the results of both calculations overlap at the 2 sd level.

The second method to test for disturbance of the argon in minerals is by carrying out incremental heating experiments. Pristine undisturbed systems will give identical ages for each temperature step within error, allowing the calculation of a plateau age over most of the gas released during the experiment. In favorable cases, excess argon can be recognised from anomalously high ages in the first steps, and ages decreasing to a plateau in the higher-temperature steps. The effects of weathering of the biotite may also cause disturbance of the gas release, preventing the calculation of a plateau age. The age spectrum of MCA-1 shows an excellent plateau of over the total gas release (Fig. 9). The age spectrum of MCA-2a is somewhat disturbed both at the low-temperature end and at the high-temperature end of the experiment. Nevertheless, the experiment allows the calculation of a plateau age that meets commonly accepted criteria (Fleck et al., 1977).

However, multiple single fusion ages, plateau ages and isochron ages of the biotites are inconsistent and neither match the stratigraphic order. Furthermore, we note that there is a potential problem with excess argon as documented from the plagioclase analyses.

7. Discussion and conclusions

7.1. Integrated stratigraphic framework

The results of the planktonic foraminiferal biostratigraphic analysis confirm the cyclostratigraphic and tephrastratigraphic correlations between the Monte del Casino subsections and between the Monte del Casino composite section and Monte Tondo (Fig. 3). The Monte del Casino sapropel pattern and planktonic foraminiferal events can straightforwardly be correlated to previously studied sections on Crete and Gavdos (Fig. 10). The correlations show that the same succession of (first-order) bio-events can be recognised as elsewhere in the Mediterranean (see also Sierro et al., 1993). The consistency of the cyclostratigraphic and biostratigraphic correlations indicate that — in agreement with the field evidence — the succession in the Monte del Casino composite section is (nearly) continuous. All sapropels, bio-events and ash layers can thus be astronomically dated since the sedimentary cycles in the other sections were already calibrated to astronomical target curves (Hilgen et al., 1995; see also Fig. 10). This calibration reveals that — like in the other sections — grey beds and less prominent sapropels correlate with insolation maxima that are reduced in amplitude due to interference of precession and obliquity. The aberrantly thick cycle 29 represents a double cycle, i.e. a cycle which contains an extra cycle that lacks lithological expression.

Our correlations also demonstrate that second-

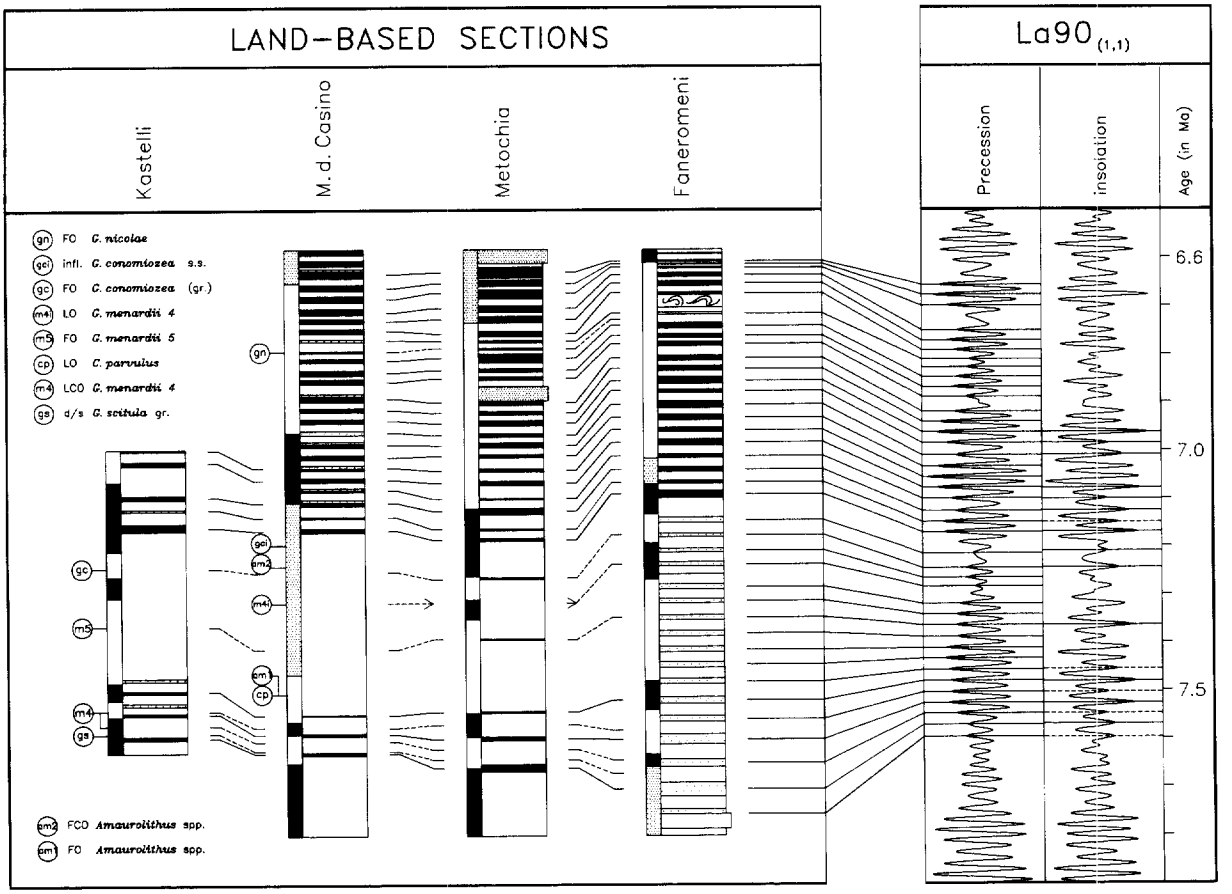

Fig. 10. Cyclostratigraphic and (planktonic foraminiferal) correlations of the Monte del Casino section to previously studied sections on Crete and Gavdos. Also shown are the correlations of the sedimentary cycles (sapropels, grey beds) to astronomical target curves (precession and 65°N lat. summer insolation) derived from solution La90 (Laskar et al., 1993; see Hilgen et al., 1995 and Lourens et al., 1996).

order events such as changes in coiling direction and short-term influxes can be very helpful to enhance the temporal resolution of biostratigraphic correlations on at least a regional (Mediterranean) scale. For instance, the last short influx of *G. menardii 4* within the range of *G. menardii 5* has been detected also in the Potamida and Faneromeni sections on Crete, and is astronomically dated at 7.28 Ma (Table 2). The (second) influx of the *G. conomiozea* group, dominated by conical types, below C18 has been reported from below the same correlative sapropel in the Potamida section (Zachariasse, 1979). The astronomical age of this influx is 7.19 Ma. Apparently, this very short influx — as well as the first influx — has been missed in other sections because of a too low sample resolution. It shows that the replacement of *G. menardii 5* by the *G. conomiozea* group is a more suitable biostratigraphic criterion to define the T/M than the FO of dominant *G. conomiozea* types (Krijgsman et al., 1995). Moreover, our results from Monte del Casino show that both boundary criteria actually result in the same position for the T/M boundary because keeled globorotaliids in the first sample containing the *G. conomiozea* group are already dominated by conical shells. Thus far, this coincidence has not been reported from other T/M

Table 2
Stratigraphic position and astronomically derived ages for calcareous plankton events in the Monte del Casino section (age 1) and comparison with astronomical ages for the same events according to Hilgen et al.'s (1995) age 2

No.	Species	Event	Level (m)	Age range	Age 1	Age 2
Planktonic forams:						
8	*G. nicolae*	FO	28.11–28.35	6.822–6.832	6.827	6.829
7	*G. conomiozea*	influx	17.01	–	7.192	–
6	*G. conomiozea* gr.	FRO	15.28–15.46	7.236–7.241	7.239	7.240
5	*G. menardii 4*	influx	13.63	–	7.289	*7.280*
4	*G. menardii 5*	FO	10.77–10.89	7.367–7.371	7.369	7.355
3	*C. parvulus*	LO	8.13–8.37	7.440–7.446	7.443	7.456
2	*G. menardii 4*	LCO	6.24–6.36	7.504–7.509	7.507	7.512
1	*G. scitula* gr.	d/s coiling	4.73–4.85	7.564–7.568	7.566	*7.553*
Calcareous nanno's:						
b	*Amaurolithus* spp.	FCO	15.61–15.86	7.225–7.232	7.228	–
a	*Amaurolithus* spp.	FO	8.13–8.37	7.440–7.446	7.443	–

Ages 2 in italics are based on additional biostratigraphic analysis of samples from the Faneromeni section on Crete.

boundary sections. Finally, the persistent change in coiling direction of the *G. scitula* group — from alternatingly sinistral/dextral to sinistral — might prove to be a useful bio-event in the Mediterranean.

Most of the planktonic foraminiferal events are useful for (time-)stratigraphic correlations on a regional scale, but are less suitable for correlations on a wider preferably global scale although certain events can easily be recognised in the adjacent Atlantic (Sierro et al., 1993; Hodell et al., 1994). An event with a potential for global correlations is the FO of *Amaurolithus* spp. In the present study, this event is found below ash 104. Comparison with magnetostratigraphically well-constrained sections (Fig. 10) shows that event is slightly younger than the younger end of C3Br.2n. In a previous study of the Monte del Casino section, Negri and Vigliotti (1997) reported the first rare *Amaurolithus* from a lower level, approximately 1 m below ash 102. This would correspond to a position within C4n.1n, which is slightly older than the oldest occurrence of this genus reported from the equatorial Pacific (Raffi et al., 1995; Shackleton et al., 1995). Moreover, the rare and discontinuous occurrence of *Amaurolithus* in the early part of its range makes the FO (of *Amaurolithus*) less-suitable for long-distance time-stratigraphic correlations.

The magnetostratigraphy, on the other hand, is only partly consistent with the cyclostratigraphic and biostratigraphic correlations. Positions of the polarity reversals recorded in the lower part of the section [C4n.1n(y), C3Br.2n(o) and C3Br.2n(y)] are in good agreement with the results from the Metochia section on Gavdos, but show a consistent offset of $\frac{1}{2}$–1 sedimentary cycle compared to the position in the Faneromeni and Kastelli sections on Crete (Fig. 6). This offset was earlier explained by diagenetic processes causing a delay in NRM acquisition (Van Hoof et al., 1993). The position of the reversal recorded in the upper part of the section [C3Bn(y)] is well defined in cycle C25, i.e. 4–5 cycles younger than its position observed on Gavdos and Crete. Delayed acquisition processes can certainly not explain the younger age found at Monte del Casino because sedimentary remanence acquisition mechanisms can make the reversal appear older, but not younger. Remarkably, the difference between astronomical ages of polarity reversals and the ages according to CK95 is exceptionally large (166 kyr) for C3Bn(y) (Hilgen

et al., 1995). A position at cycle C25 in Monte del Casino will significantly reduce this discrepancy to approximately 70 kyr.

7.2. Comparison of Ar/Ar ages and astronomical ages

The astronomical ages of sapropels and ash layers are obtained independently from radiometric dating methods and can be compared with our $^{40}Ar/^{39}Ar$ ages from Monte del Casino. Our data were calculated against USGS standard TCR sanidine with an age of 27.92 Ma. In the Amsterdam laboratory, we measured an age of 28.09 ± 0.10 Ma for the FCT-3 biotite (Wijbrans et al., 1995). Previous argon datings on the Monte del Casino ashes have been reported by Vai et al. (1993) and Laurenzi et al. (1997) who used the FCT-3 biotite, at an age of 27.55 ± 0.08 Ma (Lanphere et al., 1990), as their principal standard. When comparing our data with those of Laurenzi et al., we would expect an offset between the two data sets caused by these different results on the FCT-3 biotite. We recalculated Laurenzi et al.'s argon ages from Monte del Casino to an age of 28.09 Ma for FCT-3 biotite to ensure a meaningful comparison with our data (Table 3).

To ensure a meaningful comparison with the astronomical ages, all $^{40}Ar/^{39}Ar$ ages should in addition be corrected for the cross-calibration of radioisotopic and astronomical time (Renne et al., 1994; Hilgen et al., 1997). Hilgen et al. showed that the best fit between $^{40}Ar/^{39}Ar$ ages — of biotites and feldspars, including sanidine — and astronomical ages of two ash beds from Greece is obtained when the ages of the mineral dating standards TCR sanidine and FCT-3 biotite are slightly increased by 20–60 kyr. Renne et al. (1994) reported an increase of 110 (or 190) kyr in the age of dating standards (their FCT sanidine) when comparing $^{40}Ar/^{39}Ar$ and astronomical ages for seven polarity reversals younger than 3.5 Ma. This increase is reduced to 40 kyr if slightly modified astronomical ages of Pliocene reversal boundaries (Lourens et al., 1996) are taken into account (see also Hilgen et al., 1997). We refrained, however, from recalculating all $^{40}Ar/^{39}Ar$ ages because of the minor corrections necessary and uncertainties in the exact intercalibration between radioisotopic and astronomical time.

Comparing the $^{40}Ar/^{39}Ar$ ages with the astronomical ages, it shows that the weighted mean ages of the plagioclase are without exception too old. This is caused by excess argon since isochron ages are younger. Discrepancies with the single fusion ages of biotite are smaller and range from -180 to $+350$ kyr. Comparison of the astronomical ages with the (younger) biotite isochron ages does not result in a reduction of the discrepancies (-330 to $+190$ kyr). The plateau age of MCA-2a is in good agreement with the astronomical age, whereas the plateau age of MCA-1, which shows a much better age spectrum, is not. Our plateau age of MCA-1 can also be compared with the plateau age of ash 102 of Laurenzi et al. (1997), which shows that these ages obtained by two different laboratories are only slightly different (Table 3).

Chemical analyses by Laurenzi et al. (1997) on the Monte del Casino biotite crystals show that chemical alteration of the biotite can be excluded because the potassium content is high in all samples. Furthermore, homogeneous compositions of the biotite in most ashes indicate that contamination by detrital components can be neglected.

In conclusion, the comparison with the astronomical ages shows that the $^{40}Ar/^{39}Ar$ datings on the Monte del Casino biotites are not suitable for accurately dating the sedimentary succession — and hence the T/M boundary — even if statistically acceptable ages are obtained. Moreover, these datings do not match the stratigraphic order and their reproducibility is poor since weighted mean ages of total fusion, isochron ages and plateau ages are inconsistent. Nevertheless, they gave a good approximation of the age of the section with an average and maximum deviation of 0.16 and 0.36 Myr, respectively.

7.3. The Monte del Casino section: a potential T/M boundary stratotype?

Vai et al. (1993) have argued that de Monte del Casino section is a suitable GSSP for the T/M boundary. The excellent correlation between this section and time-equivalent sections on Crete and

Table 3
Astronomically derived ages of ash layers and comparison with $^{40}Ar/^{39}Ar$ ages

Samplecode	Ashlayer	Astronomical age		Mineral	This study		Laurenzi et al. (1997)	
		1	2		$^{40}Ar/^{39}Ar$	isochron	plateau	isochron
	108	6.874						
MCA-9	107	7.040		biotite	7.30±0.05	7.27±0.06	7.16±0.03	7.15±0.04
				plagioclase	7.89±0.07	8.17±0.08		
	106a	7.101						
	106	7.239	7.241				7.42±0.04	7.37±0.19
MCA-3	105	7.308	7.299	biotite	7.70±0.03	7.27±0.08	7.55±0.04	7.50±0.06
				plagioclase	7.48±0.05	7.41±0.04		
	104b	7.360	7.347					
	104a	7.414	7.406					
	104	7.426	7.419					
MCA-2a	103	7.539		biotite	7.49±0.01	7.51±0.03		
				B-plateau	7.56±0.07	7.51±0.02		
				plagioclase	9.55±0.07	7.17±0.09		7.08
	102c	7.548						
	102b	7.562						
A	102a	7.581	7.575					
MCA-1	102	7.589	7.579	biotite	7.53±0.01	7.30±0.10		
				B-plateau	7.48±0.02	7.58±0.05	7.42±0.04	7.41±0.04
				plagioclase	8.34±0.12	7.46±0.18		
b	100f	7.608	7.589					
MCA-0	100e	7.615	7.593	biotite	7.47±0.02	7.32±0.15		
D	100d	7.636	7.604					
E	100c	7.643	7.608					
F	100b	7.658	7.616					
G	100a	7.661	7.618					
H	100	7.681	7.628					

To ensure a meaningful comparison, all radiometric ages are recalculated to an age of 28.09 Ma for the FCT biotite. The first astronomical age (age 1) was obtained by linear interpolation of the sedimentation rate between astronomically dated calibration points, i.e. the sapropel mid-points (see Hilgen et al., 1995 for exact ages). Ages of ash layers older than sapropel 15 were calculated in this way (the preliminary log and biostratigraphy show that sapropel 13 is found 14.35 m below sapropel 15 and that this sapropel corresponds to sapropel K7/M68/G79 in Hilgen et al., 1995) and by linear downward extrapolation of the sedimentation rate taking the stratigraphic distance from sapropel 15 to 16 in the Casino 3 subsection as starting point (age 2). These age of the ash layers is expected to fall within the calculated age range because of a downward increase in sedimentation rate. The second age (age 2) of ash layers intercalated between sapropel 17 and 18 was calculated by including additional age calibration points based on (the position of) certain bio-events (FO *G. menardii 5*, last influx *G. menardii 4* and FO *G. conomiozea*) which have been dated astronomically in the continuously cyclically bedded Faneromeni section. The ages are considered more reliable because this approach corrects (in a thick homogeneous interval) for intra-formational changes in sedimentation rate, disturbances in stratigraphic thicknesses as a consequence of tectonic deformation and inaccuracies in logging exact stratigraphic distances.

Gavdos indicates that the Monte del Casino section is continuous, without tectonic complications or stratigraphic hiatuses in the boundary interval. These correlations provide a set of astronomical ages for all sedimentary cycles, ash layers and bio-events in the Monte del Casino section (Tables 2 and 3).

This indicates that the Monte del Casino remains a candidate stratotype section for the T/M boundary. The large number of ash layers could be an extra recommendation, but they are not suitable for an accurate and precise dating of the boundary. A more serious short-coming is the poor paleomagnetic signal in the critical interval. However, the boundary is magnetostratigraphically well-constraint in sections on Crete and occurs within chron C3Br.1r (Krijgsman et al., 1995). A final concern is the permanence of exposure. The (natu-

ral) outcrop has changed considerably during the last years (R. Calieri, pers. commun. and own field observations) and there is at present no guarantee that the section is long lasting.

In conclusion, the Monte del Casino section remains a possible GSSP for the T/M boundary, but its qualities as a boundary stratotype should be critically weighted against those of other candidate sections. This evaluation, however, is beyond the scope of the present paper.

Acknowledgements

We thank Gian Vai and Roberta Calieri for discussing the Monte del Casino section in the field. Gerrit van 't Veld and Geert Ittman processed the micropaleontological samples. Henk Meijer assisted with the paleomagnetic measurements. The presence of Lucas Lourens in the field was of crucial importance because without his ability in constructing tents it would have been impossible to have sampled the section in the rain and mud. The reviews of W. Lowrie, D. Rio and M.A. Lanphere are gratefully acknowledged. Francesca e Benedetto del Albergo "Richi" (Borgo Tossignano): *mille grazie per i vini buoni e i pranzi buonissimi.* This study was partly supported by The Netherlands Geosciences Foundation (GOA) with financial aid from the Netherlands Organisation of Scientific Research (NWO) and the EU HCM program. This is MIOMAR contribution 5.

References

Benson, R.H., Rakic-El Bied, K., Bonaduce, G., 1991. An important current reversal (influx) in the Rifian corridor (Morocco) at the Tortonian—Messinian boundary: the end of Tethys ocean. Paleoceanography 6, 164–192.

Benson, R.H., Rakic-El Bied, K. et al.1995. The Bou Regreg section, Morocco: Proposed Global Boundary Stratotype Section and Point of the Pliocene. Notes Mém. Serv. Géol. Maroc 383, 1–93.

Bukry, D., 1973. Low-latitude coccolith biostratigraphic zonation. In: Edgar, N.T., Saunders, J.B. et al. (Eds.), Initial Reports of the Deep Sea Drilling Project, Vol. 15. U.S. Gov. Print. Off., Washington, DC, pp. 685–703.

Calieri, R., 1992. Stratigrafia, analisi paleoclimatica e radiometria del Tortoniano superiore Messiniano preevaporitico in Appennino Romagnolo (M. del Casino—M. Tondo). Thesis, Univ. Bologna, Bologna, 79 pp. (Unpubl.)

Cande, S.C., Kent, D.V., 1992. A new Geomagnetic Polarity Time Scale for the Late Cretaceous and Cenozoic. J. Geophys. Res. 97, 13917–13951.

Cande, S.C., Kent, D.V., 1995. Revised calibration of the Geomagnetic Polarity Time Scale for the Late Cretaceous and Cenozoic. J. Geophys. Res. 100, 6093–6095.

Colalongo, M.L., di Grande, A., d'Onofrio, S., Gianelli, L., Iaccarino, S., Mazzei, R., Poppi Brigatti, M.F., Romeo, M., Rossi, A., Salvatorini, G., 1979. A proposal for the Tortonian—Messinian boundary. Ann. Géol. Pays Hellén., Tome hors Sér. 1979, Fasc. I, pp. 285–294.

Cowie, J.W., Ziegler, W., Boucot, A.J., Basset, M.G., Remane, J., 1986. Guidelines and Statutes of the International Commission on Stratigraphy (ICS). Courier Forschungsinst. Senckenberg 83, 1–14.

Dekkers, M.J., 1989. Magnetic properties of natural pyrrhotite, II. High- and low-temperature behaviour of Jrs and TRM as function of grain size. Phys. Earth Planet. Inter. 57, 266–283.

Dodd, B., Anderson, V.B., 1994. Design, construction, commissioning, and use of a new Cd lined incore irradiation tube for the Oregon State University TRIGA Reactor. OSU Reactor Center, Corvallis, OR, Intern. Rep.

Fleck, R.J., Sutter, J.F., Elliot, D.H., 1977. Interpretation of discordant $^{40}Ar/^{39}Ar$ age spectra of Mesozoic tholeiites from Antarctica. Geochim. Cosmochim. Acta 41, 15–32.

Hilgen, F.J., Krijgsman, W., Langereis, C.G., Lourens, L.J., Santarelli, A., Zachariasse, W.J., 1995. An astronomical (polarity) time scale for the late Miocene. Earth Planet. Sci. Lett. 136, 495–510.

Hilgen, F.J., Krijgsman, W., Wijbrans, J.R., 1997. First direct comparison of astronomical and $^{40}Ar/^{39}Ar$ ages of ash beds: potential implications for the age of mineral dating standards. Geophys. Res. Lett. (submitted).

Hodell, D.A., Benson, R.H., Kent, D.V., Boersma, A., Rakic-El Bied, K., Magnetostratigraphic, biostratigraphic, and stable isotope stratigraphy of an Upper Miocene drill core from the Salé Briqueterie (northwest Morocco): A high-resolution chronology for the Messinian stage. 1994. Paleoceanography 9, 835–855.

Kissel, C., Barrier, E., Laj, C., Lee, T.Q., 1986. Magnetic fabric in undeformed marine clays from compressional zones. Tectonics 5, 769–781.

Krijgsman, W., Hilgen, F.J., Langereis, C.G., Zachariasse, W.J., 1994. The age of the Tortonian/Messinian boundary. Earth Planet. Sci. Lett. 121, 533–547.

Krijgsman, W., Hilgen, F.J., Langereis, C.G., Santarelli, A., Zachariasse, W.J., 1995. Late Miocene magnetostratigraphy, biostratigraphy and cyclostratigraphy in the Mediterranean. Earth Planet. Sci. Lett. 136, 475–494.

Langereis, C.G., Dekkers, M.J., 1992. Paleomagnetism and rock magnetism of the Tortonian—Messinian boundary stratotype at Falconara, Sicily. Phys. Earth Planet. Inter. 71, 100–111.

Langereis, C.G., Zachariasse, W.J., Zijderveld, J.D.A., 1984. Late Miocene magnetobiostratigraphy of Crete. Mar. Micropaleontol. 8, 261–281.

Lanphere, M.A., Sawyer, D.A., Fleck, R.J., 1990. High-resolution $^{40}Ar/^{39}Ar$ geochronology of Tertiary volcanic rocks, Western U.S.A. Geol. Soc. Aust., Abstr. 27, 57

Laskar, J., Loutel, F., Boudin, F., 1993. Orbital, precessional, and insolation quantities for the Earth from −20 Myr to +10 Myr. Astron. Astrophys. 270, 522–533.

Laurenzi, M., Tateo, F., Villa, I.M., Vai, G.B., 1997. New radiometric datings bracketing the Tortonian/Messinian boundary in the Romagna potential stratotype sections (Northern Apennines). In: Montanari, A., Odin, G.S., Coccioni, R. (Eds.), Miocene Integrated Stratigraphy. Elsevier, Amsterdam (in press).

Lourens, L.J., Hilgen, F.J., Zachariasse, W.J., van Hoof, A.A.M., Antonarakou, A., Vergnaud-Grazzini, C., 1996. Evaluation of the Pliocene to early Pleistocene astronomical time scale. Paleoceanography 11, 391–413.

Lowrie, W., 1990. Identification of ferromagnetic minerals in a rock by coercivity and unblocking temperature properties. Geophys. Res. Lett. 17, 159–162.

Martini, E., 1971. Standard Tertiary and Quaternary calcareous nannoplankton zonation. In: Farinacci, A. (Ed.), Proc. II Planktonic Conf. Rome, 1970, 2, 739–785.

Mullender, T.A.T., Van Velzen, A.J., Dekkers, M.J., 1993. Continuous drift correction and separate identification of ferrimagnetic and paramagnetic contributions in thermomagnetic runs. Geophys. J. Int. 114, 663–672.

Negri, A., Vigliotti, L., 1997. Calcareous nannofossil biostratigraphy and paleomagnetism of the Monte Tondo and Monte del Casino sections (Romagna Appennine, Italy). In: Montanari, A., Odin, G.S., Coccioni, R. (Eds.), Miocene Integrated Stratigraphy. Elsevier, Amsterdam (in press).

Perch Nielsen, K., 1985. Cenozoic calcareous nannofossils. In: Bolli, H.B., Saunders, J.B., Perch Nielsen, K. (Eds.), Plankton Stratigraphy. Cambridge Univ. Press, Cambridge, pp. 427–555.

Raffi, I., Rio, D., d'Atri, A., Fornaciari, E., Rocchetti, S., 1995. Quantitative distribution patterns and biomagnetostratigraphy of middle and late Miocene calcareous nannofossils from equatorial Indian and Pacific Oceans (Legs 115, 130 and 138). Proc. Ocean Drill. Prog., Sci. Results 138, 479–503.

Renne, P.R., Deino, A.L., Walter, R.C., Turrin, B.D., Swisher, C.C., Becker, T.A., Curtis, G.H., Sharp, W.D., Jaouni, A.R., 1994. Intercalibration of astronomical and radioisotopic time. Geology 22, 783–786.

Rio, D., Raffi, I., Villa, G., 1990. Plio-Pleistocene calcareous nannofossil distribution patterns in the Western Mediterranean. In: Kastens, K.A., Mascle, J. et al. (Eds.), Proceedings of the Ocean Drilling Program, Scientific Results, Vol. 107. Ocean Drill. Prog., College Station, TX, pp. 513–553.

Roberts, A.P., 1995. Magnetic properties of sedimentary greigite (Fe_3S_4). Earth Planet. Sci. Lett. 134, 227–236.

Scheepers, P.J.J., 1994. Tectonic rotations in the Tyrrhenian Arc system during the Quaternary and late Tertiary. Geol. Ultraiectina 112, 350

Shackleton, N.J., Baldauf, J.G., Flores, J.-A., Iwai, M., Moore, T.C., Raffi, I., Vincent, E., 1995. Biostratigraphic summary for Leg 138. Proc. Ocean Drill. Prog., Sci. Results 138, 517–533.

Sierro, F.J., The replacement of the "*Globorotalia menardii*" group by the "*Globorotalia miotumida*" group: An aid to recognizing the Tortonian/Messinian boundary in the Mediterranean and adjacent Atlantic. 1985. Mar. Micropaleontol. 9, 525–535.

Sierro, F.J., Flores, J.A., Civis, J., González Delgado, J.A., Francés, G., 1993. Late Miocene globorotaliid event-stratigraphy and biogeography in the NE-Atlantic and Mediterranean. Mar. Micropaleontol. 21, 143–168.

Skinner, B.J., Erd, R.C., Grimaldi, F.S., 1964. Greigite, the thio-spinel of iron: A new mineral. Am. Mineral. 50, 1487–1489.

Spender, M.R., Coey, J.M.D., Morrish, A.H., 1972. The magnetic properties and Mössbauer spectra of synthetic samples of Fe_3S_4. Can. J. Phys. 50, 2313–2326.

Vai, G.B., Laurenzi, M., 1994. Radiometric dating of the Tortonian/Messinian boundary (N. Apennines, Italy). ICOG-8 (8th Int. Conf. Geochronol. Cosmochronol. Isot. Geol.), Berkeley, CA, Abstr.

Vai, G.B., Villa, I.M., Colalongo, M.L., 1993. First radiometric dating of the Tortonian/Messinian boundary.. C.R. Acad. Paris. 316 (2), 1407–1414.

Van Hoof, A.A.M., van Os, B.J., Rademakers, J.G., Langereis, C.G., de Lange, G.J., 1993. A paleomagnetic and geochemical record of the upper Cochiti reversal and two subsequent precessional cycles from southern Sicily (Italy). Earth Planet. Sci. Lett. 117, 235–250.

Van Velzen, A.J., 1993. Thermal alteration of magnetic sulphides in marine marls from the Vrica section and the influence on the demagnetization of the natural remanent magnetization. . Geol. Ultraiectina 122, 109–145.

Wijbrans, J.R., Pringle, M.S., Koppers, A.A.P., Scheveers, R., 1995. Argon geochronology of small samples using the Vulkaan argon laserprobe. Proc. Kon. Ned. Akad. Wetensch. 98 (2), 185–218.

Zachariasse, W.J., 1979. The origin of *Globorotalia conomiozea* in the Mediterranean and the value of its entry level in biostratigraphic correlations. Ann. Géol. Pays. Hellén., Tome hors Sér., Fasc. III, VIIth Int. Cong. on Mediterranean Neogene, Athens, pp. 1281–1292.